Taylor & Francis
Taylor & Francis Group

Vehicle System Dynamics
International Journal of Vehicle Mechanics and Mobility

ISSN: (Print) (Online) Journal homepage: www.tandfonline.com/journals/nvsd20

An overhead line virtual test track for the assessment of railway catenary pantograph interaction

Sam Hayes & David I. Fletcher

To cite this article: Sam Hayes & David I. Fletcher (25 Jul 2024): An overhead line virtual test track for the assessment of railway catenary pantograph interaction, Vehicle System Dynamics, DOI: 10.1080/00423114.2024.2382745

To link to this article: https://doi.org/10.1080/00423114.2024.2382745

Published online: 25 Jul 2024.

VEHICLE SYSTEM DYNAMICS
https://doi.org/10.1080/00423114.2024.2382745

An overhead line virtual test track for the assessment of railway catenary pantograph interaction

Sam Hayes and David I. Fletcher

Department of Mechanical Engineering, University of Sheffield, Sheffield, UK

ABSTRACT

This paper presents the infrastructure geometry of a virtual test track for investigating the dynamic performance of train pantographs and overhead line systems with discrete features including height transitions and overlaps. This has been developed to support cascade of legacy fleets to new regions of the rail network and to better understand how legacy electrification infrastructure can support more modern fleets. The geometry is developed as an 'obstacle course' representative of overhead line fitted to legacy routes which have been electrified after their initial construction and is reusable across overhead line equipment types and modelling packages. A range of demonstration results are presented to illustrate application of three pantograph models. The virtual test track geometry and dynamic modelling can be used to assess the performance of catenary/pantograph combinations for overhead line geometries with discrete features and large height variations that are not currently covered by validation methods such as described in BS EN50318. The approach is applicable as a planning tool to establish safe working speeds across a range of overhead line features when full overhead line geometry is not available, or will be too costly to obtain, in the context of extending the utilisation of legacy assets.

ARTICLE HISTORY
Received 27 November 2023
Revised 2 July 2024
Accepted 16 July 2024

KEYWORDS
Electrification; railway infrastructure; catenary/pantograph interaction; dynamics; test track

1. Introduction

Successful rail electrification using overhead line systems depends on mechanical and electrical compatibility of the catenary and pantograph operating as a system. For completely new build systems this is largely achieved through ensuring standards compliance on both sides of the interface [1,2]. But for legacy infrastructure and cascade of legacy fleets to new areas of the rail network, the process is much less straightforward. Typically, a legacy fleet and older infrastructure on which it runs will not comply with new-build interoperability standards, but they will have been tuned over time to work well together. To support the cascade of legacy fleets and to better understand how legacy electrification infrastructure can support more modern fleets there is a need to model dynamic compatibility and safe working speeds across a range of overhead line features that may be found on a route. In this paper, we define a standard reusable overhead line geometry including features representative of legacy infrastructure allowing the dynamic performance of overhead line

CONTACT David I. Fletcher d.i.fletcher@sheffield.ac.uk

and pantograph systems to be tested and compared. The approach has a similarity to the 'benchmarking' process defining a virtual test track that has been undertaken previously for vehicle dynamics assessment [3,4]. An example implementation is demonstrated but the geometry may be deployed in any modelling package.

Modelling of catenary pantograph dynamics has significantly advanced in the 2000s through the use of simulation techniques such as Finite Element Analysis coupled with lumped-mass or multibody pantographs models [5–8]. These have much greater capability than numerical approaches used historically for which only idealised overhead line geometries could be considered [9,10]. Validation of numerical approaches is typically undertaken using either measured data from real-world installations [11–13] or through comparison against reference model data as described in BS EN50318 (2018) [14]. In complying with the EN50318 standard the expected tolerances in modelling predictions are tighter against the reference model than for real-world data to take account of variabilities in real-world systems such as inexactly constructed overhead line geometry and wind loading. However, the geometry in the standard excludes many features characteristic of retro-fit electrification such as low clearance tunnels and wire height changes at road crossings. In this paper, we go beyond the sample geometry presented in BS EN50318 by defining a virtual overhead line test track formed of five tension lengths with discrete features developed to assess the dynamic compatibility of OLE geometries with various pantograph types and configurations. The modelling work is prefaced with a validation of the simulation software according to the BS EN 50318 (2018) methodology in Section 1.1. This is to provide confidence in subsequent predictive applications. A high-level description of the virtual test track geometry is provided in Section 2, and further details are available in the Supplementary Data (https://doi.org/10.15131/shef.data.24632322.v2). In Section 3 example pantograph models are described for use with the virtual infrastructure to demonstrate its application, with results and conclusions given in Sections 4 and 5, respectively. While the results for the cases modelled are useful in themselves, the broader aim is to demonstrate the applicability and reusability of the virtual test track geometry. Using the details provided here assessment can be conducted for any fleet and overhead line system with the preferred modelling package and pantograph models of the infrastructure manager or vehicle operator.

1.1. Modelling methodology

The virtual test track was designed with typical features of installed legacy or retrofitted overhead line, including large-scale height changes, overlaps between tension lengths, and fitted or free-running bridge types. The exact geometry can be modified to accurately reflect the system design for the OLE under consideration, e.g. alteration of the stagger, permissible wire gradients or system height (also known as the encumbrance, the distance between the catenary wire and the contact wire at its suspension points). To demonstrate the application of the virtual test track several combinations of OLE type and pantograph configuration were simulated at train speeds between 120 and 200 km/h. These serve to demonstrate how the infrastructure defined reveals the limiting features and locations for which deployment of a fleet may breach acceptable OLE defection or forces, reflecting also GB rail operation where the current maximum linespeed is 200 km/h.

All modelling was performed using the simulation software PCaDA v6 [11] developed by Politecnico di Milano, and in accordance with BS EN50367 (Criteria to achieve technical compatibility between pantographs and overhead contact line) [15] with the raw data passed through a 20 Hz low-pass filter before statistical analysis was performed. The model generates force and displacement data for locations along the line and through time for the passage of a pantograph. While plotting these directly can be useful to visualise the behaviour, the extensive data defining these curves are very difficult to compare between cases or against criteria defining acceptability of the OLE and pantograph combination. Reduction is therefore required for which the following metrics and acceptability criteria were used:

1. The ratio of the contact force standard deviation (σ) to the arithmetic mean of the contact force (F_m) should be less than or equal to 0.3, taking these acceptability criteria from BS EN50367 [15]. This acceptability threshold for σ/F_m gives a probability that less than 0.27% of the contact force occurrences are less than $0.1F_m$ therefore avoiding contact loss.
2. The contact wire uplift should not exceed 50% of the design uplift for the overhead line equipment, taking this definition of acceptability from BS EN50119 (Railway applications, fixed installations, electric traction overhead contact lines) [16].

An important factor when using these metrics is that there is no judgement made on the quality of the equipment under examination. The judgement is about suitability for duty at a particular line speed and configuration.

1.2. Model demonstration runs undertaken

To demonstrate the capabilities of the overhead line geometry to reveal locations of criteria exceedance and limiting speeds for acceptable operation, results are presented of simulations with 'Series 1' overhead line equipment [17] and three pantograph types: the Brecknell Willis (BW) High Speed (HSA), BW Low Height Mk1 (HSP Mk1) and BW Low Height Mk2 (HSP Mk2) (further details of these pantographs are in Section 3). Depending on train configuration, for example, the joining of two or more multiple-unit trains, or double-headed locomotive-hauled trains, there are a range of separations at which pantographs may operate within a single train. This is important for system dynamics as a second or third pantograph will run on a contact wire which is already displaced and oscillating from the passage of the leading pantograph. These examples of multi-pantograph cases therefore represent the most restrictive operational cases at which allowable running speeds are expected to be below that of a single pantograph train. The combinations of pantograph types, numbers and positions are given in Table 1. These are a subset of 124 combinations of OLE types and pantograph configurations modelled for the development of industry guidance on OLE to pantograph compatibility [18]. In application of the virtual test track any combination of pantograph types and separation can be explored. The example cases here were defined by real train configurations running in Great Britain rather than aiming to identify optimum spacings or types.

Table 1. Pantograph types and configurations used for simulation with the Series 1 equipment.

Pantograph type	Number of pantographs	Pantograph spacing[a] (m)	Maximum speed[b] (km/h)
BW HSA	1	–	200
	2	75	To be determined
	2	86	
	3	81/75	
	Double headed	8	
BW HSP Mk1	1	–	160
	2	75	To be determined
	2	86	
	3	81/75	
	Double headed	8	
BW HSP Mk2	1	–	175
	2	75	To be determined
	2	86	
	Double headed	8	
HSX250	1	–	200
	2	200	200

[a]A spacing of 81/75 corresponds to 81 m between the front and middle pantograph and 75 m between the middle and rear.
[b]Speeds for single pantograph operation determined in previous works [18], are included here to allow for comparison with multiple pantograph operation.

1.3. Model validation of PCaDA v6 against BS EN50318 (2018)

Although earlier versions of PCaDA have undergone validation [11] against the 2002 release of BS EN50318 this standard has since been updated with an improved validation procedure [14]. The updated PCaDA was certified by Italcertifier as compliant with BS EN50318 (2018) in 2023, but in addition to this a validation a check was performed on the specific code used in the current work (PCaDA version 6). Compliance with the standard was assessed for train speeds of 275 and 320 km/h, and for two-pantograph operation with a pantograph spacing of 200 m. Although this speed range exceeds that of interest for the virtual test track it is a requirement for the standard validation procedure. For the validation simulations, statistical analysis of the simulated contact force was performed and compared with the reference statistical output provided in the BS EN50318 (2018) standard.

The simulated raw force data for the validation was filtered according to BS EN50367 using a sixth-order filter with a cut-off frequency of 20 Hz. For the statistical analysis, the contact force standard deviation was evaluated across three frequency ranges: (a) 0–20 Hz, the entire range of interests, (b) 0–5 Hz, the span passing frequency, and (c) 5—20 Hz, the dropper passing frequency.

Table 2 gives the statistical output for the validation testing of PCaDA and the permissible bands provided by BS EN50318 (2018). For each of the assessment criteria, the modelling output is within the required ranges and therefore can be considered valid according to the methodology.

2. Virtual test track geometry

To facilitate re-usability of the virtual test track this section gives a high-level description of the infrastructure layout developed to assess the compatibility of different pantograph configurations and OLE designs. A detailed description of the wire heights, support positions and dropper positions and lengths is available in the Supplementary Data. The detail

Table 2. Statistical output and uplift measurements for the compliance cases at 275 and 320 km/h.

		Pantograph 1		Pantograph 2	
275 km/h		EN50318 Range	PCaDA	EN50318 Range	PCaDA
Mean	N	141.5–146.5	143	141.5–146.5	144
Standard deviation (0–20 Hz)	N	31.9–34.8	33.5	50–54.5	53.1
Standard deviation (0–5 Hz)	N	26.4–28.9	27	41.2–45.4	45.1
Standard deviation (5–20 Hz)	N	16.2–22.4	22	25.2–34.7	30.9
Maximum	N	219–244	229	241–290	250
Minimum	N	71–86	86	14–50	43.3
Vertical position range	mm	38–49	42.2	53–70	62.2
Maximum uplift at support	mm	39–48	41.6	45–54	47.8
Contact loss	%	0	0	0	0
		Pantograph 1		Pantograph 2	
320 km/h		EN50318 Range	PCaDA	EN50318 Range	PCaDA
Mean	N	166.5–171.5	170	166.5–171.5	169
Standard deviation (0–20 Hz)	N	49.5–62.9	52.7	30.2–43.8	43.1
Standard deviation (0–5 Hz)	N	38.7–44.4	41.3	14.3–23.3	22.9
Standard deviation (5–20 Hz)	N	29–46.2	36.7	26.7–38.2	36
Maximum	N	295–343	296	252–317	262
Minimum	N	55–82	65.3	21–86	55.5
Vertical position range	mm	39–51	47.8	18–35	27.2
Maximum uplift at support	mm	57–64	60	50–61	54.2
Contact loss	%	0	0	0	0

geometry is in this case calculated for the Furrer + Frey Series 1 overhead line equipment and follows its System Description manual [19]. A similar translation from a high-level layout to a detailed design within the requirements of the system could be conducted for any other overhead line system.

Figure 1 gives a schematic of the virtual test track with nominal wire heights for the catenary and contact wires. Note compression of the track position axis relative to vertical wire height by a factor over 300 leads to the appearance of steeper wire gradients than will exist in reality. The virtual test track represents a high speed line of tangent track without curves, and includes (features are labelled A–E):

- Running in and out sections 600 m long (A) that are composed of 10 uniform simple catenary 60 m spans to account for end effects and bringing the pantograph into contact with the OLE.
- Five tension lengths giving four overlaps (B). The tension lengths can be made arbitrarily long in the modelling software; however, realistic tension length is limited by wire manufacture and system design for thermal expansion compensation, so the system design maximum of 1500 m has been used here.
- A reduction in the contact wire height from the nominal 4.7–4.2 m representing an overbridge (C). To achieve the contact wire height changes, the maximum design gradient has been adopted of 1:625, with transition spans between changes in wire gradient of 1:1250.
- A wire height increase from 4.2 to 5.8 m (D) to approximate the effect of a transition from a bridge to a road level crossing at the maximum permissible gradient, followed by a return to the nominal wire height of 4.7 m.

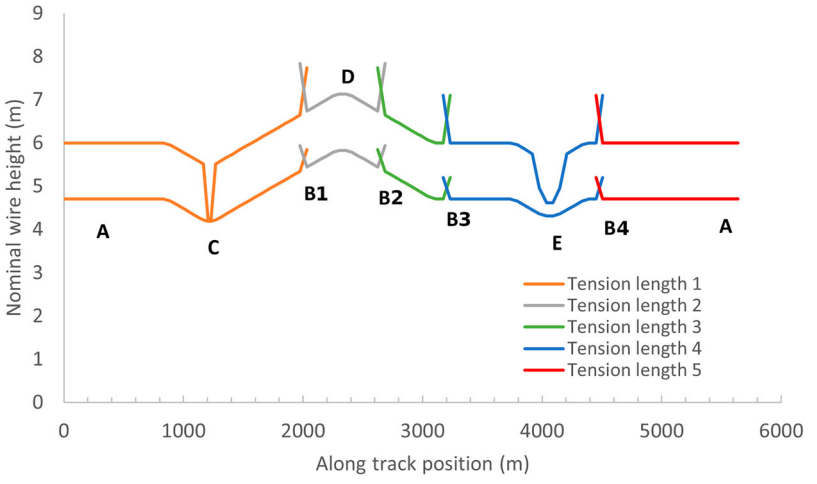

Figure 1. Virtual test track schematic. Droppers omitted for clarity.

Table 3. Series 1 dropper positions and spacings for single span overlaps.

Overlap span length (m)	Number of droppers	Dropper spacing (m)	Dropper position from in running structure (m)	
			D_1	D_2
55	2	11.00	5.50	16.50
56		11.25		16.75
58		11.75		17.25
60		12.25		17.75

- A smaller wire height reduction is also included, from 4.7 to 4.4 m (E) and then returns to the nominal wire height of 4.7 m for the remainder of the test track.
- Contact wire presag of 1000th of the span length is included apart from in overlap spans where there is no presag and the contact wire is uplifted at its natural rise.

Stagger was omitted from the track geometry, however, can be included in the OLE geometry according to the system equipment being considered. Typical values for Series 1 equipment are 230 mm on tangent track and 320 mm on curved track. On curved tracks, it is noted that a good stagger design is needed to restrict large lateral forces on curves [20]; however, the focus here was on the vertical forces.

Between each tension length, conventional overlap geometry has been adopted. In the case of Series 1, the overlaps are single span without anchor spans, but for another system, the specifics could be changed according to design standards for that system. Along the length of the span the out-of-running contact wire height increases by 0.5 m and the system height increases from 1.3 to 1.9 m. The dropper positions for the single-span overlaps are given in Table 3 and a schematic of the wire arrangement is given in Figure 2.

Dropper spacing for non-overlap spans is calculated according to Appendix 1, and the dropper lengths for the test track are provided in the Supplementary Data to this paper.

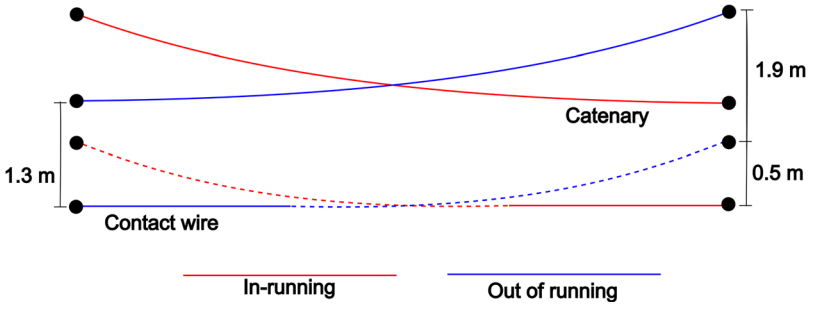

Figure 2. Schematic of a single span overlap for traffic moving left to right. At the first structure, the system height is 1.3 m for the out-of-running wire. Along the length of the span, the out-of-running contact wire height increases by 0.5 m to the second structure and the system height increases to 1.9 m. Geometry of the in-running wires follows a similar pattern.

Table 4. Conductor particulars for Series 1 equipment.

Contact wire	Conductor identification	BS EN50149: AC-120 CuAg
	Tension	16.5 kN
	Linear mass	1.07 kg/m
Catenary wire	Cross-sectional area	65 mm^2
	Material	DIN 48201 BzII
	Tension	13 kN
	Diameter	10.5 mm
	Conductor arrangement	19/2.1 mm
	Linear mass	0.6 kg/m

The effective mass of each dropper was taken to be 0.93 kg/m and the dropper clamps have a mass of 0.115 kg. As with the other values, this would be modified for other OLE systems.

At the first overbridge (Point C), the system height reduces to zero, and a twin contact arrangement supported by bridge arms is used to represent low clearance fitted bridges widely used on the GB network. The second bridge (E) uses a free-running bridge arrangement with conventional cantilevers and a reduced system height of 200 mm. At Point C, the bridge arm stiffness is calculated according to $k = GJ/L$, where G is the shear modulus of the bridge arm, $J = \pi D^4/32$, is the torsional constant and L is the arm length. For a glass fibre bridge arm, $G = 3.6$ GPa, $D = 36$ mm and $L = 1665$ mm, therefore the stiffness of the bridge arm is, 3.57 kN/m. The effective mass of the bridge arm is 0.5 kg. For other registration points, the registration arm was modelled as a point mass with an effective mass of 0.9 kg and stiffness of 1 kN/m.

For the Series 1 equipment, the contact and catenary wire particulars are given in Table 4. The contact wire is formed of copper–silver (CuAg) wire with a cross-sectional area of 120 mm^2 and the catenary wire is formed of 19 bronze II (BzII) 2.1 mm diameter strands with a cross-sectional area of 65 mm^2.

3. Pantograph specification

The pantograph model is separate to the virtual test track geometry and can be selected freely by the user to simulate particular traffic. In the demonstration cases presented here widely accepted rail industry lumped-mass models of three different pantographs are used.

Table 5. Parameter values for each of the BW pantographs used for simulating the catenary pantograph interaction.

Parameter		HSA	HSP Mk1	HSP Mk2
Mass (kg)	m_1	3.42	3.53	3.53
	m_2	7.0	7.5	7.5
	m_3	8.6	7.5	5.14
Damping (Ns/m)	c_1	39.4	32.6	32.6
	c_2	0	0	0
	c_3	5	80	110
Stiffness (N/m)	k_1	26.3	0	0
	k_2	7800	7000	7000
	k_3	3000	3500	3500
Aerodynamic uplift (Ns^2/m^2)	F_a'	0.006	0.006	0.006
Static uplift (N)	F_s	90	90	90

If additional behaviours of particular equipment were of interest such as lateral roll of the pantograph then a model capturing this [21] could be used instead. To demonstrate the catenary/pantograph interaction across the virtual test track a three-lumped-mass model (Figure 3) was used to approximate the pantograph dynamics with parameter values derived from experimental identification of the pantograph dynamic characteristics [22] summarised in Table 5.

For each of the pantographs, the experimental identification of the dynamic characteristics is such that each parameter does not correspond to individual pantograph components and could be distributed in different ways to achieve similar dynamic performance [5]. For the HSP Mk1 and Mk2 pantographs where a null stiffness between the pantograph base and lower mass is given, system damping ensures that force variations due to a change in the pantograph height are captured. The use of three-lumped-mass models has been demonstrated to sufficiently capture the pantograph dynamics undergoing large-scale height changes [23,24].

Contact between the pantograph and the contact wire is determined using the penalty method with a contact stiffness k_s between the two contact surfaces of 50 kN. Vertical motion due to train movement on the suspension was not considered and the base of the pantograph is assumed to be vertically and laterally fixed relative to the track. Lateral displacement of the pantograph (e.g. due to pantograph sway or lateral aerodynamics) was not considered.

4. Model demonstration results and discussion

In general, it is expected that pantograph to contact wire force and registration arm uplift will rise with increased train speeds. By testing the combinations of pantograph and overhead line system across a range of speeds the maximum permissible operating speed and locations of excessive force or uplift can therefore be established, giving confidence to operate a fleet prior to introduction to a new route. This section details the model demonstration results graphically for uplift force and displacement for a range of pantograph types with the Series 1 overhead line equipment design. For each of the combinations, statistical output is provided in Appendix 2. Modelling was performed using a 9th generation Intel Core i5-9400F processor with typical model run times to assess each combination around

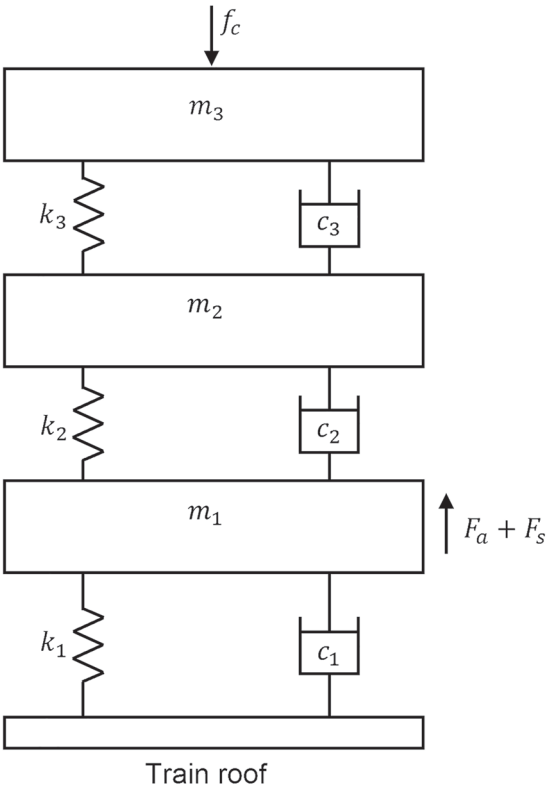

Figure 3. Three-lumped-mass pantograph model adopted for the modelling. Each of the m_i, c_i and k_i correspond to mass, damping and stiffness values for each of the considered pantographs, f_c is the contact force and F_a and F_s correspond to the aerodynamic and static uplift forces. The aerodynamic uplift, F_a, is calculated according to $F_a = F'_a v^2$, where v. is the train speed in m/s.

90 min, with the option for parallel simulation in PCaDA allowing for all the considered train speeds to be simulated simultaneously.

4.1. Pantograph contact wire uplift force

Results in terms of the compatibility criteria (ratio of contact force standard deviation (σ) to arithmetic mean of the contact force (F_m)) used to assess the interaction between two HSA pantographs with different spacings is given in Figure 4(a). As expected, there is a trend to rising values at higher speeds, with non-linearity in the response across speeds reflecting the complex non-linear nature of the pantograph suspension in combination with the overhead line stiffness changes throughout the virtual test track. In all cases, the focus here is on multiple pantograph configurations as dynamic interaction of the pantographs limits operational speed to below that allowable with a single pantograph, and it's particularly relevant to multiple unit service provision.

Judging using the σ/F_m assessment criteria, for the cases considered the highest speed compatible is for the greatest separation of the front and rear pantographs. This improved dynamic performance of the system depends on two factors: (i) time for the mechanical

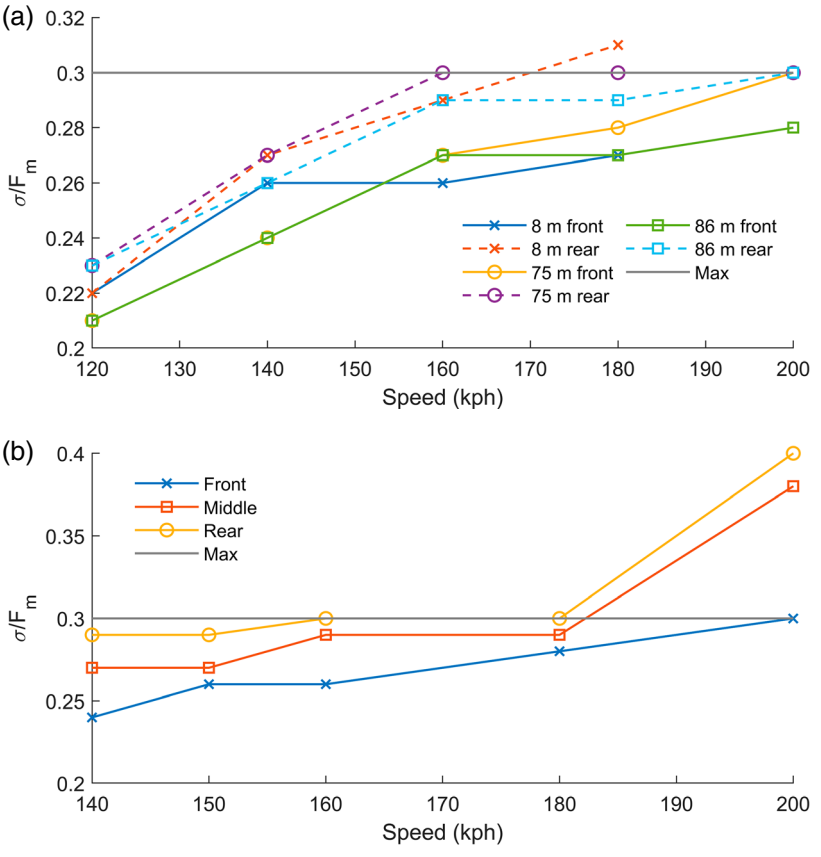

Figure 4. The EN50367 criteria (σ/F_m) used to assess compliance for the combinations of (a) two pantograph operation at separations of 8, 75 and 86 m, and (b) three pantograph (81/75 m separation) HSA operation with the Series 1 equipment. Legend indicates the pantograph under consideration and spacing. The maximum allowable operating limit is shown as max.

wave due to the front pantograph to decay before the second pantograph passes, which increases with pantograph separation, and (ii) the pantograph separation as a proportion of contact wire motion wavelength, as discussed in Section 4.2. Note the specific separations are set by the train configurations considered so are not infinitely variable and will vary with the train type considered. The force variability results for rear pantographs (dotted lines) all exceed those for the front pantographs, a behaviour which is present in the other results discussed below. When the pantograph spacing was 8 m, the maximum compliant speed for the front and rear considered together was predicted to be 160 km/h, which increased to 200 km/h with the larger spacings considered. The compliant speed is effectively determined by the rear pantograph as this reaches the limit at a slower speed. The difference in dynamic performance due to the small increase in pantograph spacing from 75 to 86 m was marginal with maximum compliant speeds of 200 km/h in both cases, and the performance of the rear pantograph with the smaller spacing was approximately 7% worse for the 15% increase in pantograph spacing. Comparing all of the two pantograph cases at 160 km/h, σ/F_m was in the range 0.29–0.30 in all cases, indicating that at compliant

speeds, pantograph spacing has little impact on the dynamic performance of the system, however increasing the spacing yields higher permissible speeds for the same pantograph type.

Whilst pantograph spacing for the same pantograph type has a marginal effect on the dynamic performance at compliant speeds, the addition of a third pantograph is predicted to drive a reduction in compliant speeds. In this case, the spacing was chosen to represent a particular multiple-unit train configuration giving spacing of 81 m (front to middle pantograph), and 75 m (middle to rear pantograph). As can be seen in Figure 4(b), the maximum compliant speed for the three-pantograph case is 180 km/h, limited by the rear pantograph, compared with 200 km/h for both the 75 and 86 m spacing. Whilst in the two-pantograph case, only the dynamic effect of the leading pantograph acts on the trailing pantograph, the rear pantograph during three-pantograph operation is subject to the mechanical waves due to the two leading pantographs driving a greater degradation of the dynamic performance. Comparing the rear pantographs in the two and three pantograph cases, the dynamic performance at 200 km/h would be approximately 33% worse if allowed to operate at this speed with a third pantograph (σ/F_m parameter rises from 0.3 to 0.4).

Figure 5(a) gives the assessment criteria for the Series 1 equipment with two HSP Mk1 pantographs. As with the HSA pantograph type, the larger spacing yields a higher compliant speed. The effect of reducing spacing from 75 to 86 m is again shown to be marginal with both spacings achieving the same compliant speed when simulated with the virtual test track. The double-headed arrangement with a separation of only 8 m between the front and rear pantographs is only compliant up to 160 km/h due to the increased dynamic effect of the leading pantograph on the trailing pantograph. For larger pantograph spacings, it is unlikely that the light damping of the OLE [25] has mitigated the contact wire oscillation amplitude sufficiently to reduce dynamic effects, as these typically persist well after the passage of the train.

As for the HSA pantograph, the three pantograph HSP Mk1 case (Figure 5(b)) shows that the rear pantograph becomes the limiting factor, reducing compliant speed to 180 kph. Were the operation to be pushed to 200 kph the dynamic force parameter is lower than for the HSA case at that speed, but would still exceed the 0.3 limit imposed by BS EN 50367. It is not currently known how significant this exceedance would be in terms of reduction in equipment life or increased risk of dewirements or whether these worsen in proportion to the parameter or worsen severely and non-linearly. There is further research required in understanding the impacts of non-compliance to enable a cost–benefit analysis to fully assess the technical limitations in comparison to the potential for additional service provision in cases of marginal criteria exceedance. Given the nature of the virtual test track, it is expected that marginal criteria exceedance will be driven by specific gradients in the overhead line, typically at overlaps. In finely balanced cases a bespoke dynamic analysis for the actual geometry of a route could provide additional insight if it is thought the virtual test track represents an over stringent test.

The sensitivity of outcomes to the pantograph design is shown in the data plotted in Figure 6. Moving from the Mk1 to Mk2 version of the HSP pantograph enables compliance with the BS EN 50367 force criteria across the full speed range up to 200 kph for all pantograph separations tested with one or two pantographs. This should not be taken to indicate that particular equipment is better or worse, but that it is designed for and suited to different duties.

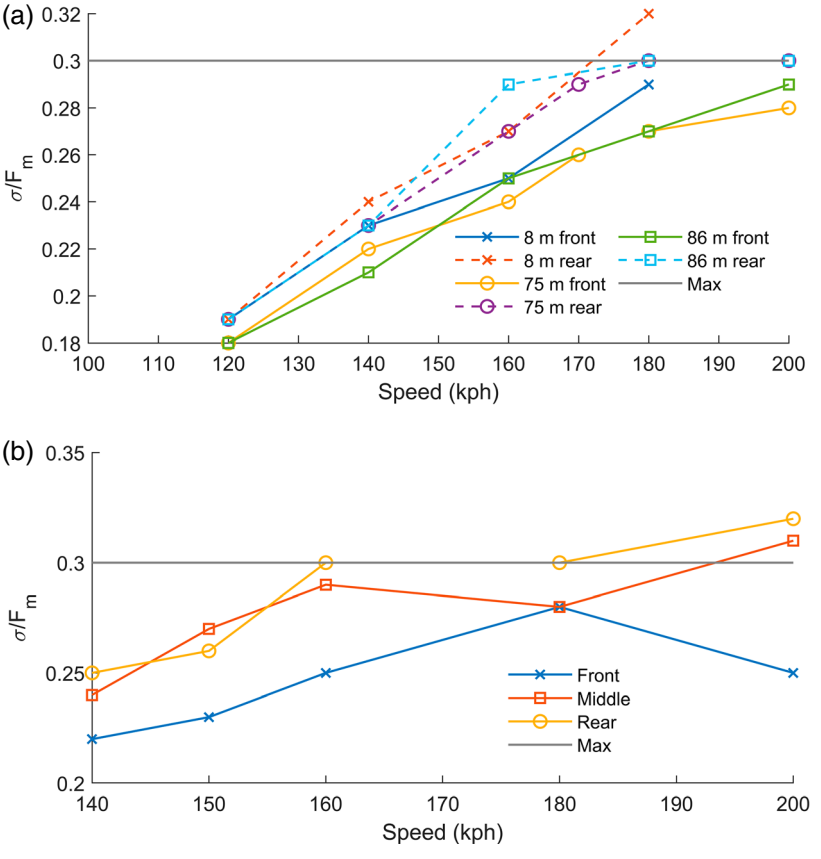

Figure 5. The EN50367 criteria (σ/F_m) used to assess compliance for the combinations of (a) two pantograph operation, and (b) three pantograph HSP Mk1 operation with the Series 1 equipment. Legend indicates the pantograph under consideration and spacing.

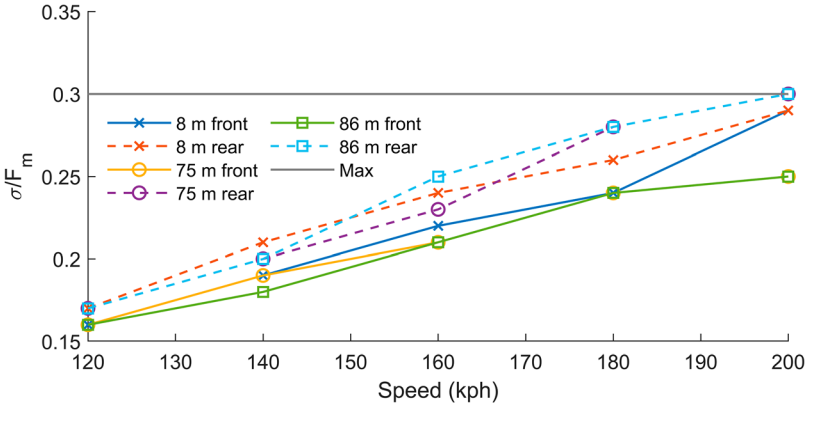

Figure 6. The EN50367 criteria (σ/F_m) used to assess compliance for the combinations of two HSP Mk2 pantograph operation with the Series 1 equipment. Legend indicates the pantograph under consideration and spacing.

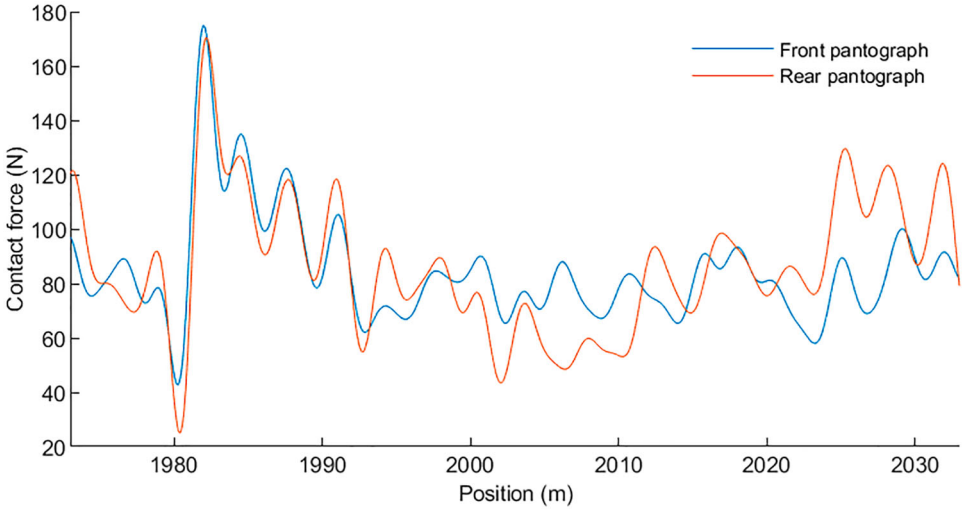

Figure 7. Force traces for pantograph positions through the ascending overlap for the HSA pantograph at 200 km/h between the start and end of the overlap span at 1973 and 2033 m.

Figure 7 shows the contact force traces for two HSA pantographs at 200 km/h for the ascending overlap between tension lengths one and two (Position B1 in Figure 1). At the beginning of the span, both pantographs experience a larger contact force due to the increased vertical stiffness at the registration arm at 1980 m, and similar force patterns are observed until the pantographs contact both the in- and out-of-running wires. At the twin contact point, a divergence between the front and rear pantograph force patterns is observed (approximately 2000 m in the Figure) with larger force variability predicted for the second pantograph.

For the descending overlap (Location B2 in Figure 1), results in Figure 8 show both pantographs also experience a large contact force due to the increased vertical stiffness at the registration arm at 2626 m. Moving into the span, the contact force decreases as the pantograph moves down following the path of the out-of-running contact wire. Towards the midspan ($\sim$ 2650 to 2660 m) where the pantograph is in contact with both the in- and out of running wires a larger contact force variability is predicted.

The descending overlap has a marginally worse dynamic performance compared to the ascending overlap. The contact force standard deviation for the trailing pantographs (typically the poorest dynamically) within the overlap spans was 22 N (ascending) and 23 N (descending). The discrete performance of the overlaps was also similar with respect to the maximum contact forces predicted. The discrete force maxima for the ascending and descending spans were predicted to be 172 and 161 N, respectively, with the ascending overlap contact approximately 5.6% higher.

To further explore the effect of overlaps Figure 9 shows the force traces for the level overlap B4 in Figure 1 and the force traces for a comparable case on the Network Rail Melton Rail Innovation and Development Centre (RIDC) test track. The track positions in the figure refer to those at RIDC while the modelled geometry at Location B4 has been translated from its position within the model. The data are not expected to show exact agreement because (i) installed overhead line geometry is always an imperfect implementation of the

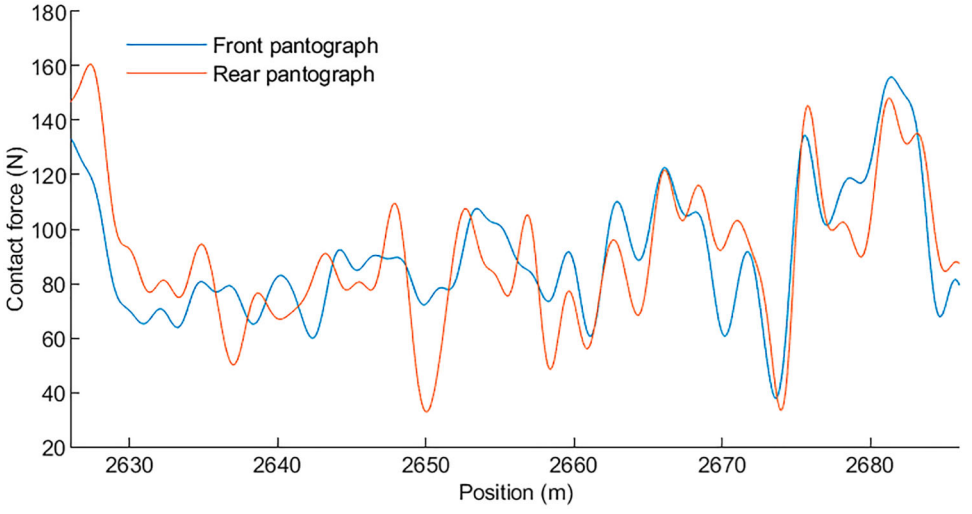

Figure 8. Force traces for pantograph positions through the descending overlap span running between 2626 and 2686 m for the HSA pantograph at 200 km/h.

design, (ii) wind flow at the test track is not represented in the model, and (iii) the test train used an instrumented pantograph for which exact mass distribution is unknown but is compared here with data for pantograph type HSA. Despite these complications, the comparison of data is still informative with the simulations and track data revealing the same characteristics. For the leading pantograph in the middle span of the overlap where the pantograph is in contact with two contact wires ($\sim$1360 to 1390 m), both the measured and simulated data indicate an increase in the contact force above that in the spans either side when the pantograph is running only on a single contact wire. The trailing pantograph shows greater variability in force in both model and test track data, for example, both reaching very low contact forces at a track position of 1430 m. The rear pantograph also reaches higher contact forces (in the range 190–200 N) than the leading pantograph (in the range 170–180 N) in both simulation and track test data. This greater range of forces at the rear pantograph would be expected from the data discussed above for leading and trailing pantographs at the ascending and descending overlaps.

4.2. Support arm uplift

Support arm uplift predictions were made at discrete locations through the virtual test track for the maximum permissible speed according to the EN50367 criteria shown in the previous section. These locations were:

- Within the ascending overlap between tension lengths 1 and 2 at 1973 m
- Either side of the maximum nominal wire height, either side of the level crossing (in tension length 2 at 2302 and 2357 m)
- Within the descending overlap between tension lengths 2 and 3 at 2686 m
- In the nominal level section after the level crossing (in tension length 3 at 3350 m)
- In the level section after the final overlap (in tension length 5 at 4739 m).

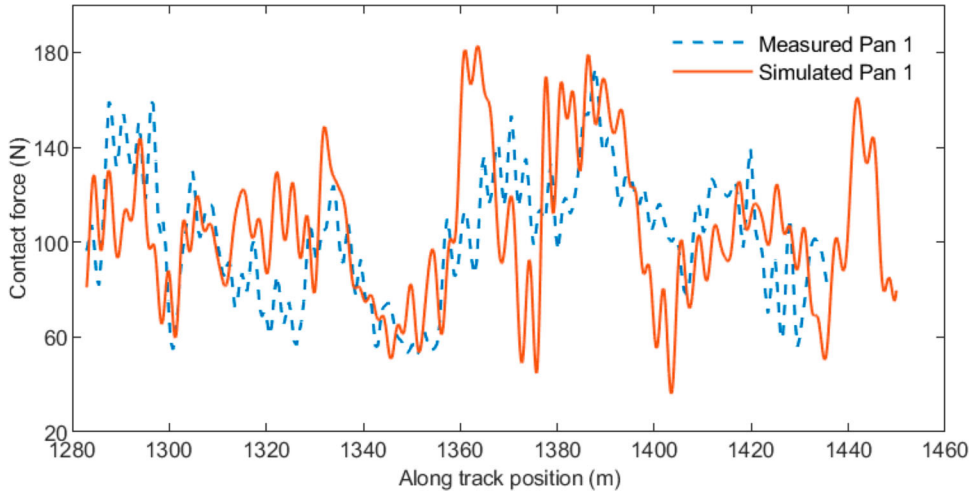

(a) Leading pantograph contact force through a level overlap.

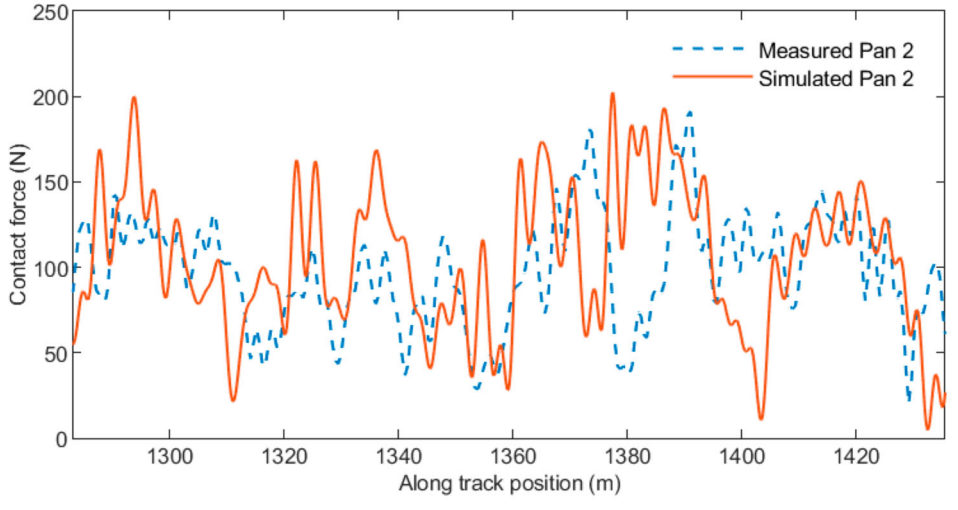

(b) Trailing pantograph contact force through a level overlap.

Figure 9. Comparison of contact force traces for (a) leading and (b) trailing pantographs between measured track data and overlap B4 in Figure 1. Track positions are based on the measured track data, with modelled cases translated to align the overhead line geometry. (a) Leading pantograph contact force through a level overlap. (b) Trailing pantograph contact force through a level overlap.

From Figure 10, the largest uplifts for each pantograph type are predicted to occur at the first overlap for the in-running wire (position 1973 m). At this location, due to the dropper arrangement in a single span overlap (shown in Figure 2) the contact wire vertical stiffness is reduced and therefore allows for a greater wire uplift compared with standard spans. In each case, these highest uplifts were predicted for the 8 m pantograph spacing despite this having the lowest permissible speed. This is thought to be caused by the trailing pantograph uplifting an already uplifted contact wire as this separation at 160 km/h leaves only

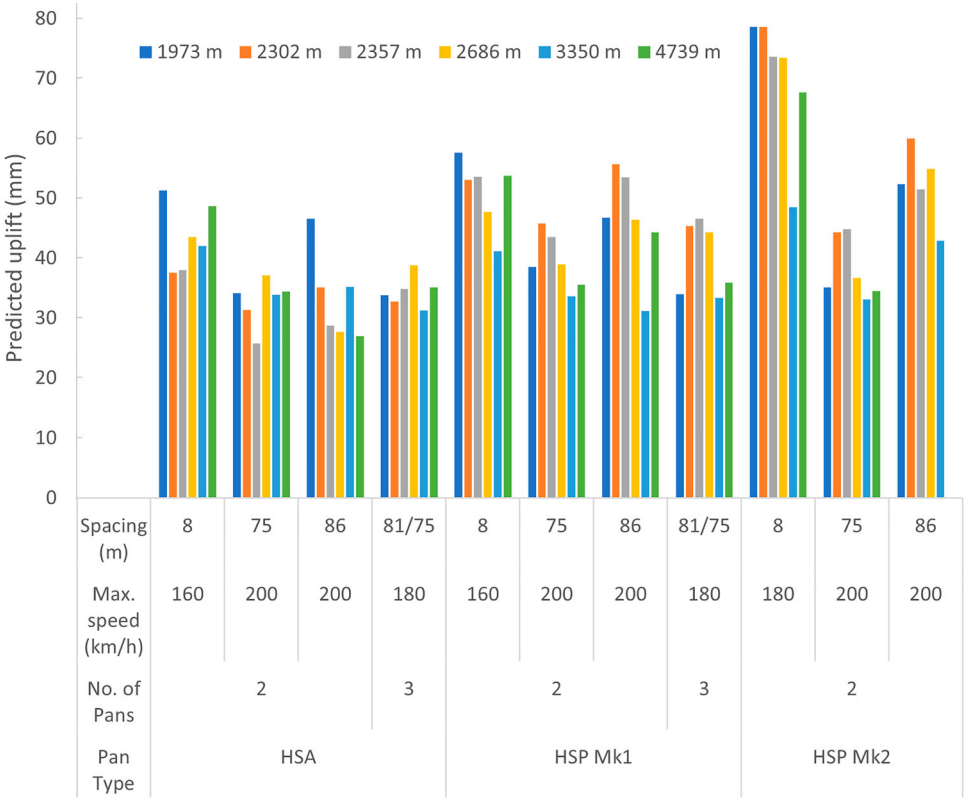

Figure 10. Maximum support arm uplift at locations throughout the obstacle course for each of the pantograph configurations and Series 1 equipment. Each uplift measurement corresponds to the maximum permitted speed according to the statistical analysis and is compared against a maximum design uplift of 200 mm.

0.18 s for the wire to return from its raised position. Since overhead line systems are almost always very lightly damped the wire will oscillate with degreasing amplitude rather than returning directly from its raised position. For larger pantograph spacings, the contact wire displacement amplitude will have reduced from its maximum before the arrival of subsequent pantographs, and a reduced maximum uplift is found from the model. However, the oscillation of the wire gives the potential for resonance or periodicity in this behaviour as the natural wavelength of wire oscillation interacts with the pantograph spacing such that the later pantograph may tend to contact at a node or anti-node. This will be highly dependent on configuration (wire tension, train speed, pantograph separation). In applying the model to a particular line and fleet these must all be explored to identify, for example, the potential for resonant contact wire deflections below a speed at which smooth low wire deflection running is predicted.

Despite the effect described above for the 8 m pantograph spacing, across all of the cases assessed it was found that train speed is not a dominant driver of uplift. For any particular overhead line geometry, the predicted uplift depends largely on the pantograph type and spacing. In both the HSP Mk1 and Mk2 cases, both the 75 and 86 m spacings attained a permissible speed of 200 km/h, however, the 86 m spacing was predicted to have approximately

33% (Mk1) and 37% (Mk2) higher contact wire uplifts across all of the measured locations. For the HSA pantograph, the choice between the larger spacings was predicted to have no significant influence on the contact wire uplift, with average uplifts of 33 mm for both 75 and 86 m spacings. For the 86 m pantograph spacing, all three pantograph types were compliant up to 200 km/h with the HSP Mk2 type predicted to achieve the highest average wire uplifts of 52 mm compared with 33 (HSA) and 46 mm (HSP Mk 1).

5. Conclusions

For new build railway systems standards compliance can be assured, supporting both mechanical and electrical compatibility of the catenary and pantograph operating as a system. However, for efficient rail operation, there is often a need to cascade legacy fleets to new areas of the network or to run new trains on old infrastructure that is not compliant with recent standards. Being able to model compatibility of overhead line and pantograph systems ahead of time is a valuable planning tool, but in many cases, full overhead line geometry will not be available or will be costly to obtain.

This paper presents a virtual test track 'obstacle course' developed to assess the compatibility of different pantograph configurations and overhead line equipment types. Features included are typical of retro-fit electrification on GB infrastructure but are relevant to any electrification of older infrastructure with low clearance bridges/tunnels, and road crossings. Besides this application, the virtual track infrastructure geometry also provides a new research tool for comparison of modelling software in its representation of discrete overhead line features such as large contact wire height changes that are not covered by existing validation methodologies such as the reference model in BS EN50318 (2018).

The modelling software used for the demonstration of the obstacle course was validated against the existing methodology for a standard simple catenary. It showed good standards of compliance with all modelling output within the required bands. The obstacle course presented here has been developed for specific cases of GB equipment types, however, within the generic features represented it can be applied in combination with design standards for almost any equipment type and for any pantograph for which dynamic characteristics are available as lumped-mass representations.

Acknowledgments

The authors would like to acknowledge support and data provided by the Rail Safety and Standards Board (RSSB) and Furrer + Frey GB throughout the project, and to Andrea Collina from Politecnico di Milano and Christoph Sieber from Furrer + Frey AG for providing support and access to the PCaDA software used for the modelling work.

Disclosure statement

No potential conflict of interest was reported by the authors.

Funding

The authors gratefully acknowledge funding provided for this work by Rail Safety and Standards Board (RSSB) as part of project T1244, Characterising the compatibility of Pantographs and Overhead Contact Systems.

References

[1] Railway interoperability national technical specification notice: Energy (ENE). Department for Transport. [cited 2021 Jan 1]. Available from: https://www.gov.uk/government/publications/railway-interoperability-national-technical-specification-notices-ntsns.

[2] Commission Regulation (EU) No 1302/2014 of 18 November 2014 concerning a technical specification for interoperability relating to the rolling stock – locomotives and passenger rolling stock subsystem of the rail system in the European Union. Available from: http://data.europa.eu/eli/reg/2014/1302/2020-03-11

[3] Iwnicki S., editor. The Manchester benchmarks for rail vehicle simulation. 1st ed. London: Routledge; 2017. doi:10.1201/9780203736425

[4] Bezin Y, Pålsson BA. Multibody simulation benchmark for dynamic vehicle-track interaction in switches and crossings: modelling description and simulation tasks. Veh Syst Dyn. 2023;61(3):644–659. doi:10.1080/00423114.2021.1942079

[5] Hayes S, Fletcher DI, Beagles AE, et al. Effect of contact wire gradient on the dynamic performance of the catenary pantograph system. Veh Syst Dyn. 2021;59(12):1916–1939. doi:10.1080/00423114.2020.1798473

[6] Beagles A, Fletcher D, Peffers M, et al. Validation of a new model for railway overhead line dynamics. Proc Inst Civ Eng: Transp. 2016;169(5):339–349. doi:10.1680/jtran.16.00020

[7] Bautista A, Montesinos J, Pintado P. Dynamic interaction between pantograph and rigid overhead lines using a coupled FEM – multibody procedure. Mech Mach Theory. 2016;97:100–111. doi:10.1016/j.mechmachtheory.2015.10.009

[8] Gonzalez FJ, Chover JA, Suarez B, et al. Dynamic analysis using finite elements to calculate the critical wear section of the contact wire in suburban railway overhead conductor rails. Proc Inst Mech Eng Pt J Rail Rapid Transit. 2008;222(2):145–157. doi:10.1243/09544097JRRT144

[9] Gilbert G, Davies HEH. Pantograph motion on a nearly uniform railway overhead line. Proc Inst Electr Eng. 1966;113(3):485–492. doi:10.1049/piee.1966.0078

[10] Levy S, Bain JA, Leclerc EJ. Railway overhead contact systems, catenary-pantograph dynamics for power collection at high speeds. Trans ASME J Eng Ind. 1968;90(4):692–699. doi:10.1115/1.3604711

[11] Collina A, Bruni S, Facchinetti A, et al. PCaDA statement of methods. Veh Syst Dyn. 2015;53(3):347–356. doi:10.1080/00423114.2014.959027

[12] Tustin A, Broomfield R. Trolley wire overhead for main line railways. Railway Gazette. 1969: 185–191.

[13] Sell RG. British railways research on current collection. Railway Gazette. 1966: 312–320.

[14] BS EN 50318:2018 + A1:2022, Railway applications. Current collection systems. Validation of simulation of the dynamic interaction between pantograph and overhead contact line. British Standards Institution [cited 2022 Jun 30]. Available from: https://knowledge.bsigroup.com

[15] BS EN 50367:2020 + A1:2022, Railway applications. Fixed installations and rolling stock. Criteria to achieve technical compatibility between pantographs and overhead contact line. British Standards Institution. [cited 2022 Oct 31]. Available from: https://knowledge.bsigroup.com

[16] BS EN 50119:2020, Railway applications. Fixed installations. Electric traction overhead contact lines. [cited 2020 Apr 30]. British Standards Institution. Available from: https://knowledge.bsigroup.com

[17] Series 1, The Great Western Electrification Project. Furrer + Frey AG, Switzerland [cited 2023 Nov 17]. Available from: https://www.furrerfrey.ch/en/systems/Series-1.html.

[18] Characterising the Pantographs and Overhead Contact Systems. Technical report T1244, Rail Safety and Standards Board, 2022. Available from: https://www.rssb.co.uk/research-catalogue/CatalogueItem/T1244

[19] Series 1 OLE System. MAN001 System description manual, Issue 5.1 DCP5e. Oct 2015, Furrer + Frey AG, Switzerland. Available from: https://www.furrerfrey.ch

[20] Antunes P, Ambrósio J, Pombo J, et al. A new methodology to study the pantograph–catenary dynamics in curved railway tracks. Veh Syst Dyn. 2020;58(3):425–452. doi:10.1080/00423114.2019.1583348

[21] Benet J, Cuartero N, Cuartero F, et al. An advanced 3D-model for the study and simulation of the pantograph catenary system. Transp Res Part C Emerg Technol. 2013;36:138–156. doi:10.1016/j.trc.2013.08.004
[22] Lump mass models for legacy pantographs on GB mainline. Rail Safety and Standards Board Limited. 2016. Available from: https://www.rssb.co.uk/research-catalogue/CatalogueItem/T1105
[23] Ambrósio J, Pombo J, Pereira M, et al. A computational procedure for the dynamic analysis of the catenary-pantograph interaction in high-speed trains. J Theor Appl Mech. 2012;50(3):681–699.
[24] Vyasarayani CP, Uchida T, Carvalho A, et al. Parameter identification in dynamic systems using the homotopy optimization approach. Multibody Syst Dyn. 2011;26(4):411–424. doi:10.1007/s11044-011-9260-0
[25] Jiang T, Rønnquist A, Song Y. A detailed investigation of uplift and damping of a railway catenary span in traffic using a vision-based line-tracking system. J Sound Vib. 2022;527:116875. doi:10.1016/j.jsv.2022.116875

Appendices

Appendix 1. Obstacle course geometry dropper spacing

The dropper spacing, d, in standard system height (1.3 m) spans is calculated according to,

$$d = \frac{S - d_1}{n - 1}, \tag{A.1}$$

where S is the span length, $d_1/2$ is the distance to the first dropper and n is the number of droppers. The number of droppers for each of the permitted Series 1 span lengths is given in Table A1. In most cases, the distance from the support to the first dropper is 11 m. Span lengths where this is not the case are also given in Table A1. The dropper lengths are given in the Supplementary Data.

Table A1. Number of droppers for a given span length.

Span length (m)	Number of droppers	Span length (m)	d_1
20–26	2	25	12
		26	13
27–40	3	38	12
		39, 40	13
41–52	4	51, 52	12
53–65	5	65	12

Note: Only span lengths where $d_1 \neq 11$ are given in the table.

Appendix 2. Series 1 and Brecknell Willis pantograph statistical data

The statistical output for each of the simulation runs for the Brecknell Willis pantographs combined with the Series 1 equipment is provided in this section.

Table A2. Statistical output for each of the pantograph speeds for the Series 1 equipment with two HSA pantographs with 8 m spacing.

Speed (km/h)	Pan	F_m	σ	$F_m + 3\sigma$	$F_m - 3\sigma$	σ/F_m	$F_{\max}$	$F_{\min}$	Loss (%)
120	Front	91.9	20.2	152.5	31.3	0.22	139	51.2	0
	Rear	91.8	21.3	161.7	33.9	0.22	139	46.2	0
140	Front	94.1	24.5	167.6	20.6	0.26	150	41.2	0
	Rear	94.1	25.3	170	18.2	0.27	153	39.2	0
160	Front	97.7	25.8	175.1	20.3	0.26	161	45.2	0
	Rear	97.8	28.8	184.2	11.4	0.29	170	35.3	0
180	Front	101	27.6	183.8	18.2	0.27	166	39.8	0
	Rear	101	30.9	193.7	8.3	**0.31**	177	0	0.19

Notes: Pantographs that fail the EN50367 pass/fail criteria are highlighted bold within the Table. All force entries are in N, the σ/F_m is dimensionless.

Table A3. Statistical output for each of the pantograph speeds for the Series 1 equipment with two HSA pantographs with 75 m spacing.

Speed (km/h)	Pan	F_m	σ	$F_m + 3\sigma$	$F_m - 3\sigma$	σ/F_m	$F_{\max}$	$F_{\min}$	Loss (%)
120	Front	92.4	19.8	151.8	33	0.21	143	55.2	0
	Rear	92.4	21.5	156.9	27.9	0.23	146	52.2	0
140	Front	94.8	22.9	163.5	26.1	0.24	153	51.2	0
	Rear	94.8	25.6	171.6	18	0.27	158	0	0.17
160	Front	97.6	26.2	176.2	19	0.27	162	44.2	0
	Rear	97.6	29.6	186.4	8.8	0.30	169	0	0.1
180	Front	101	28.6	186.8	15.2	0.28	169	0	0.15
	Rear	101	30.7	193.1	8.9	0.30	177	0	0.16
200	Front	107	31.6	198.8	9.2	0.30	178	0	0.18
	Rear	107	32.1	203.3	10.7	0.30	191	0	0.19

Notes: No cases fail the EN50367 pass/fail criteria. All force entries are in N, the σ/F_m is dimensionless.

Table A4. Statistical output for each of the pantograph speeds for the Series 1 equipment with two HSA pantographs with 86 m spacing.

Speed (km/h)	Pan	F_m	σ	$F_m + 3\sigma$	$F_m - 3\sigma$	σ/F_m	$F_{\max}$	$F_{\min}$	Loss (%)
120	Front	92.4	19.8	151.8	33	0.21	144	55.2	0
	Rear	92.4	21.3	156.3	28.5	0.23	147	51.2	0
140	Front	94.8	22.7	162.9	26.7	0.24	152	51.2	0
	Rear	94.8	24.7	168.9	20.7	0.26	258	0	0.17
160	Front	97.6	26.3	176.5	18.7	0.27	162	0	0.04
	Rear	97.6	28.7	183.7	11.5	0.29	171	0	0.2
180	Front	101	27.6	183.8	18.2	0.27	165	45.2	0
	Rear	101	29.3	188.9	13.1	0.29	177	36.2	0
200	Front	106	29.7	195.1	16.9	0.28	175	0	0.05
	Rear	106	32.3	202.9	9.1	0.30	185	0	0.16

Notes: No cases fail the EN50367 pass/fail criteria. All force entries are in N, the σ/F_m is dimensionless.

Table A5. Statistical output for each of the pantograph speeds for the Series 1 equipment with three HSA pantographs with 81/75 m spacing.

Speed (km/h)	Pan	F_m	σ	$F_m + 3\sigma$	$F_m - 3\sigma$	σ / F_m	$F_{\max}$	$F_{\min}$	Loss (%)
140	Front	94.8	23.1	164.1	25.5	0.24	154	52.2	0
	Middle	94.8	25.7	171.9	17.7	0.27	157	43.2	0
	Rear	94.8	27.3	176.7	12.9	0.29	161	39.2	0
150	Front	96.2	25	171.2	21.2	0.26	156	47.2	0
	Middle	96.2	26.5	175.7	16.7	0.27	167	37.2	0
	Rear	96.2	27.8	179.6	12.8	0.29	162	39.2	0
160	Front	97.8	26	175.8	19.8	0.26	161	45.2	0
	Middle	97.8	29.2	185.4	10.2	0.29	168	38.2	0
	Rear	97.8	29.6	186.6	9	0.30	166	36.2	0
180	Front	101	28.3	185.9	16.1	0.28	170	45.2	0
	Middle	101	29.6	189.8	12.2	0.29	184	28.2	0
	Rear	101	30.5	192.5	9.5	0.30	184	0	0.18
200	Front	104	31.5	198.5	9.5	0.30	177	44.2	0
	Middle	104	39.8	223.4	−15.4	**0.38**	193	0	1.02
	Rear	104	41.9	229.7	−21.7	**0.40**	199	0	1.64

Notes: Pantographs that fail the EN50367 pass/fail criteria are highlighted bold within the Table. All force entries are in N, the σ / F_m is dimensionless.